An Efficient Finite Element Solution of Inhomogeneous Anisotropic and Lossy Dielectric Waveguides

Yilong Lu, *Member, IEEE,* and F. Anibal Fernandez, *Member, IEEE*

Abstract—**An efficient finite element method is presented for the full wave analysis of dielectric waveguides. This method has four major features: 1) the ability to treat a wide range of dielectric waveguide problems with arbitrarily shaped cross section, inhomogeneity, transverse-anisotropy, and significant loss (or gain); 2) total elimination of spurious solutions; 3) direct solution for the (complex) propagation constant at a specified frequency; and 4) the use of only two components of the magnetic field, thus maximizing the numerical efficiency of solution. The resultant matrix eigenvalue problem is of canonical form and is solved with an efficient method, specially developed for this purpose, taking full advantage of the sparsity of the matrices. Numerical results are shown for a variety of microwave and optical waveguides including anisotropy and losses. These examples also include closed and open-bounded structures. The computational results agree very well with analytical and previously published results.**

I. Introduction

DIELECTRIC waveguides are fundamental components of optoelectronic and microwave devices and, as such, a full, accurate description of how electromagnetic waves propagate in these structures is essential. The advance of material science and fabrication technology is continuously introducing more complicated waveguide structures. Furthermore, many materials used in dielectric waveguides are anisotropic (such as $LiNbO_3$, $LiTaO_3$, and many organic materials), further complicating the theoretical analysis of the devices. Additionally, quite often, significant losses need to be taken into account, for instance, in lossy buffer layers or metal claddings of optical waveguides (as metal is highly absorbing at optical frequencies). On the other hand, fabrication costs are still high, and measuring techniques are difficult, expensive, and time consuming. There is, therefore, a great demand for more accurate and flexible computer modeling techniques which can be used for analysis and design of a wide range of waveguiding structures.

A single scalar formulation is inadequate for the inherently hybrid mode situation of anisotropic or genuinely two-dimensional inhomogeneous waveguide problems. To evaluate rigorously the propagation characteristics of inhomogeneous anisotropic waveguides, a vectorial wave analysis is necessary, with at least two field components. According to the way the problem is formulated (or to the type of eigenvalue), the formulations may be classified into two types. One type can be called frequency formulation (or simply ω-formulation), where the eigenvalue is an explicit known function of ω; the other can be called a propagation constant formulation (or simply γ-formulation), where the eigenvalue is an explicit known function of γ. One important drawback of an ω-formulation is that, for a given waveguide, it gives the frequency of each mode corresponding to a selected value of the propagation constant, while in practice the problem is usually the inverse, that is, one is interested in finding the propagation constant (possibly complex) at a specified frequency. Consequently, iterations are usually needed to solve a practical problem when using this type of formulation. In contrast, a γ-formulation solves directly for the propagation constant at a given frequency. Additionally, due to the impracticality of a proper guess for a complex propagation constant, only γ-formulations are applicable to lossy waveguide problems (or, for the same reason, to the analysis of complex modes in lossless guides).

The finite element method is one of the most versatile methods to find accurate and efficient numerical solutions to a wide range of electromagnetic field problems. However, perhaps the most serious difficulty in applying a vectorial, nodal-based finite element method to waveguide problems (or similar problems requiring a vectorial representation) is the appearance of spurious solutions [1], [2]. Although the occurrence of spurious solutions has been known for some time, and research on this topic has been extensive in recent years, the suppression of such undesirable nonphysical solutions is still a subject of great interest.

An earlier similar formulation based on the transverse components of the magnetic fields was used by Williams and Cambrell [3] to analyze surface waves in (open) isotropic dielectric waveguides. But as the equations contain terms proportional to derivatives of the permittivity, it is not really adequate for finite element solutions of waveguides of arbitrary permittivity profiles, including abrupt dielectric interfaces [4].

Several methods have been suggested over the last decade to cure the spurious problem. Apart from the penalty method [5] which, although not eliminating the spurious solutions, allows us to shift them away from the region of interest in the spectrum, other procedures attempt to remove them altogether. For example, Hayata *et al.* [6] suggested an approach in terms of only the transverse magnetic field components for

Manuscript received July 21, 1992; revised November 17, 1992.

Y. Lu is with the School of Electrical Engineering, Nanyang Technological University, Singapore 2263, Republic of Singapore.

F. A. Fernandez is with the Department of Electronic and Electrical Engineering, University College London, London, England.

IEEE Log Number 9209358.

anisotropic lossless waveguide problems. Using the divergence condition, they managed to reduce the number of components and eliminate spurious solutions, but at the cost of losing the sparsity of the matrices (rendering the method useless but for the smallest problems). The same problem is clear in their extensions of their method to diagonal anisotropic and lossy waveguide problems [7]. In their examples, a simple mesh of 153 nodes requires 27 MB memory and about 40 seconds to obtain one point in the dispersion curve using an Hitachi S-810/10 supercomputer.

Chew and Nasir [8] proposed a four component variational γ-formulation in terms of the transverse components of both electric and magnetic fields for transverse anisotropic dielectric waveguide problems. This formulation can be reduced to one in terms of only (H_x, H_y) or (E_x, E_y), but only after assuming that both transverse fields (electric and magnetic) can be described in terms of the same set of basis functions, implicitly forcing continuity on the transverse components of both electric and magnetic fields. This, of course, will not be correct in the case of abrupt dielectric interfaces. Additionally, the resultant formulation is highly sensitive to the type of element used. For instance, square elements cause the formulation to collapse.

A γ-formulation in terms of all six components of the electric and magnetic fields was proposed by Svedin [9]. Enforcing all tangential and normal interface and boundary conditions, and implicitly forcing the zero divergence condition on both electric and magnetic fields, this formulation succeeds in eliminating spurious solutions. Although it can treat the most general anisotropic materials with full permittivity and permeability tensors, it is extremely inefficient, needing all six components of the fields (the order of the matrices is then six times the number of nodes!).

Formulations based on a combination of vector and scalar potentials have also been proposed to eliminate spurious modes [10], [11]. These are ω-formulations in terms of four variables.

A completely different way of avoiding spurious solutions is the use of *edge elements* and their generalization, *tangential elements* [12], [13]. In this approach, the interpolation functions themselves are defined as vectors, and the required continuity conditions of the field components across element boundaries are automatically satisfied. This provides a neat and elegant way of solving problems involving vector fields, although its most clear applications are still in the solution of authentically three-dimensional problems. Applications have been made of this method to two-dimesional (waveguide) problems [14], [15] although this results in a rather awkward treatment of the three different components of the field vector where two components are described in terms of edge elements and the third using nodal based elements. Furthermore, in the method of Koshiba *et al.* [15], the sparsity of the matrices is lost. The method in [14] is a γ-formulation which, according to its authors, leads to real eigenvalues. Since the spectrum of solutions of (lossless and lossy) waveguides containing inhomogeneous dielectrics is, in general, complex, this formulation is incomplete. A related approach to edge elements uses *covariant-projection elements* [16]. This has been applied to solve waveguides using an ω-formulation and requiring mixed order trial functions. No standard spurious solutions appear but, in common with edge element methods, a cluster of zero-eigenvalue is found.

Most of the existing finite element formulations for the dielectric waveguide problem have been restricted to the lossless case. In particular, all ω-formulations are only of practical interest in such a case. Of the recently proposed formulations which can eliminate spurious solutions, only Hayata *et al.* [7] show explicit applications to lossy waveguide problems. However, as mentioned before, their formulation leads to dense matrices, which is a real extravagance in the use of computer resources.

In this paper, we present in detail an efficient, vectorial, variational finite element approach for the analysis of inhomogeneous, anisotropic, and lossy dielectric waveguides [17]–[19]. It can treat a wide range of dielectric waveguide problems with arbitrary cross section and inhomogeneous, transversely anisotropic and complex permittivity tensor. This formulation gives solutions directly for the (complex) propagation constant at a specified frequency and totally eliminates spurious solutions. Numerically efficiency is maximized since it only uses the two transverse components of the magnetic field. The resultant matrix eigenvalue problem is of canonical form and involves sparse, nonsymmetric (or in general, complex non-Hermitian) matrices. An efficient solver [20] has been specially developed for this problem, and allows us to treat large problems on relatively small computers. Examples are given of several types of waveguides in microwaves and optics, including open and closed boundaries, anisotropy, and loss.

II. Variational Approach

Consider a dielectric waveguide, uniform in the z-direction and of arbitrary cross section $\bar{S}$ in the $x-y$ plane as depicted in Fig. 1. The region $\bar{S}$ consists of linear dielectric materials and electric conductors. We assume that C, the boundary of $\bar{S}$, may be open or closed and, in general, it can be divided into three parts: perfect electric conductors (PEC), perfect magnetic conductors (PMC), and infinity (INF). The dielectric material in $\bar{S}$ may be arbitrarily inhomogeneous, transversely anisotropic, and lossy. We also assume that the permeability of all dielectric materials is the constant scalar μ_0 everywhere. The relative permittivity is assumed to be given by the complex tensor

$$\bar{\bar{\epsilon}}(x,y) = \bar{\bar{\epsilon}}' - j\bar{\bar{\epsilon}}'' = \begin{bmatrix} \epsilon_{xx} & \epsilon_{xy} & 0 \\ \epsilon_{xy} & \epsilon_{yy} & 0 \\ 0 & 0 & \epsilon_{zz} \end{bmatrix} \tag{1}$$

This form of the tensor $\bar{\bar{\epsilon}}$ implies that the waveguide in Fig. 1 has reflection symmetry about the z-axis; i.e., a mode propagating in the $+z$ direction is degenerate with a mode propagating in the $-z$ direction [21].

A. Elimination of Spurious Solutions

For the dielectric waveguide problem described above, the magnetic filed vector $\boldsymbol{H}$ is continuous everywhere, while

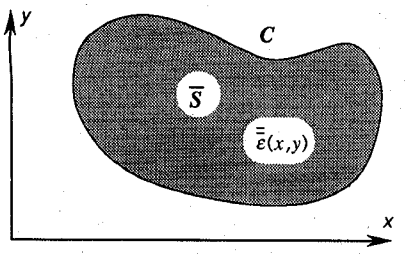

Fig. 1. The waveguide cross section.

the electric filed vector $\boldsymbol{E}$ may not be so. It is then more convenient to define the dielectric waveguide problem in terms of the magnetic field only. The double-curl equation

$$\nabla \times \left(\bar{\bar{\epsilon}}^{-1} \cdot \nabla \times \boldsymbol{H}\right) - \omega^2 \epsilon_0 \mu_0 \boldsymbol{H} = 0 \tag{2}$$

plus the tangential or the normal boundary condition have been widely adopted for the finite element analysis of the source-free dielectric waveguide boundary-value problem [2], [5]–[7]. In an analytical approach, using the above equation and one of the boundary conditions, the solenoidal character of the field solution can be guaranteed at every point in the problem domain. In that case, the tangential and normal boundary conditions are derivable from each other. This also implies that the analytical field solutions satisfy automatically the divergence equations $\nabla \cdot \boldsymbol{B} = 0$ and $\nabla \cdot \boldsymbol{D} = 0$, which are the remaining equations governing the electromagnetic field but, because of the above, it is not necessary to include them in the problem definition (2). If the complete solutions satisfy exactly the double-curl definition, it is, of course, unnecessary to include the divergence conditions. Therefore, using the double-curl definition (2) is usually sufficient to obtain the correct fields. Using numerical approximate methods, however, the situation is different. For a weak approximation as the finite element solution, the solenoidal character of the field solution cannot be guaranteed. Hence, the tangential and normal boundary conditions are no longer automatically derivable from each other, and the divergence conditions cannot be implied by the double-curl definition. As a consequence, the problem is underdetermined, and nonphysical, spurious solutions may appear.

For an $\boldsymbol{H}$-field approximation, the magnetic field double-curl equation, the magnetic field divergence condition

$$\nabla \cdot \boldsymbol{H} = 0 \tag{3}$$

and both the associated magnetic field tangential and normal boundary conditions should be used in the problem in order to eliminate spurious solutions completely.

B. Basic Differential Equation

For our dielectric waveguide problem, the permittivity tensor is assumed to have the special form (1). In that case, we can simplify the boundary-value problem definition (2) and (3) further to include only the two transverse components of the magnetic field. Denoting $\bar{\bar{\epsilon}}_{tt}$ as the 2×2 tensor

$$\bar{\bar{\epsilon}}_{tt} = \begin{bmatrix} \epsilon_{xx} & \epsilon_{xy} \\ \epsilon_{xy} & \epsilon_{yy} \end{bmatrix} \tag{4}$$

Expression (1) can be represented as

$$\bar{\bar{\epsilon}} = \bar{\bar{\epsilon}}_{tt} + \epsilon_{zz} \hat{a}_z \hat{a}_z \tag{5}$$

The double-curl equation (2) involves all three vector components of the magnetic field, while strictly only two are needed. Incorporating the divergence-free condition (3) into (2), we can reduce the number of components in the field equation to the two transverse components of the magnetic field H_x and H_y only. To achieve this purpose, we next proceed to separate the transverse and longitudinal components of (2). Here, the magnetic field is assumed to have a z dependence as $\boldsymbol{H}(x,y,z) = \boldsymbol{H}(x,y)\exp(-\gamma z)$, where γ is the (complex) propagation constant.

Equation (2) can be separated into its transverse and longitudinal parts. The transverse component of (2) becomes

$$\nabla_t \times \left(\epsilon_{zz}^{-1} \nabla_t \times \boldsymbol{H}_t\right) - \gamma \hat{a}_z \times \left[\bar{\bar{\epsilon}}_{tt}^{-1} \cdot (\nabla_t \times \hat{a}_z H_z)\right] - \omega^2 \epsilon_0 \mu_o \boldsymbol{H}_t + \gamma^2 \hat{a}_z \times \left[\bar{\bar{\epsilon}}_{tt}^{-1} \cdot (\hat{a}_z \times \boldsymbol{H}_t)\right] = \boldsymbol{0} \tag{6}$$

where $\nabla_t = \hat{a}_x \partial_x + \hat{a}_y \partial_y$, $\boldsymbol{H}_t = \hat{a}_x H_x(x,y) + \hat{a}_y H_y(x,y)$.

We can remove H_z in (6) by incorporating the divergence-free condition (3), from which we have

$$H_z = \frac{\nabla_t \cdot \boldsymbol{H}_t}{\gamma} \tag{7}$$

Substituting (7) into (6), we reduce (6) to an equation involving only the transverse magnetic field components $\boldsymbol{H}_t$, viz.,

$$\nabla_t \times \left(\epsilon_{zz}^{-1} \nabla_t \times \boldsymbol{H}_t\right) - \hat{a}_z \times \left[\bar{\bar{\epsilon}}_{tt}^{-1} \cdot \nabla_t \times (\hat{a}_z \nabla_t \cdot \boldsymbol{H}_t)\right] - \omega^2 \epsilon_0 \mu_0 \boldsymbol{H}_t + \gamma^2 \hat{a}_z \times \left[\bar{\bar{\epsilon}}_{tt}^{-1} \cdot (\hat{a}_z \times \boldsymbol{H}_t)\right] = \boldsymbol{0} \tag{8}$$

The above is an eigenvalue problem with eigenvalue γ^2. The dependence on γ^2 implies that modes with propagation factors $\exp(\pm\gamma z)$ are degenerate.

C. Local Potential Method

We can express (8) as an operator equation of the form

$$\mathcal{L}\boldsymbol{H}_t = \mathcal{A}_1 \boldsymbol{H}_t + \mathcal{A}_2 \boldsymbol{H}_t + \mathcal{A}_3 \boldsymbol{H}_t + \gamma^2 \mathcal{B} \boldsymbol{H}_t = 0 \tag{9}$$

It can be easily proved that the operator $\mathcal{L}$ in (9) is not self-adjoint. A variational expression can still be derived for this problem using the general method proposed by Chen and Lien [22], but it requires consideration of the adjoint field $\boldsymbol{H}_t^a$ which in this case, and with the usual definition of the inner product ($\langle \boldsymbol{f}, \boldsymbol{g} \rangle = \int_S \boldsymbol{f} \cdot \boldsymbol{g}\, dS$), does not correspond to the transverse magnetic field.

However, it can be observed that in expression (9), $\mathcal{A}_1, \mathcal{A}_3$, and $\mathcal{B}$ are self-adjoint operators; only $\mathcal{A}_2$ is not self-adjoint. Based on this fact, we can apply the *local potential method* [23] to (9) to obtain a variational formulation involving only $\boldsymbol{H}_t$, the transverse components of magnetic field.

Let us define $\boldsymbol{H}_t^0$ as the field at the stationary state, the solution to the problem, and assume that $\boldsymbol{H}_t$ is a value infinitesimally displaced from the stationary state. Considering

now the nonself-adjoint part of the problem, we can suppose that for such small displacement from the stationary state

$$\mathcal{A}_2 \boldsymbol{H}_t \approx \mathcal{A}_2 \boldsymbol{H}_t^0 \tag{10}$$

With this assumption, (9) becomes

$$\mathcal{L}_{\text{self}} \boldsymbol{H}_t = -\mathcal{A}_2 \boldsymbol{H}_t^0 \tag{11}$$

where $\mathcal{L}_{\text{self}} = \mathcal{A}_1 + \mathcal{A}_3 + \gamma^2 \mathcal{B}$ is a self-adjoint operator. If we now take $-\mathcal{A}_2 \boldsymbol{H}_t^0$ as a known function of position, (11) is a self-adjoint problem. We can then apply the standard methods for self-adjoint operators to (11) obtaining the variational expression

$$\begin{aligned} F(\boldsymbol{H}_t) &= \langle \boldsymbol{H}_t, \mathcal{L}_{\text{self}} \boldsymbol{H}_t \rangle + 2\langle \boldsymbol{H}_t, \mathcal{A}_2 \boldsymbol{H}_t^0 \rangle \\ &= \langle \boldsymbol{H}_t, \mathcal{A}_1 \boldsymbol{H}_t \rangle + 2\langle \boldsymbol{H}_t, \mathcal{A}_2 \boldsymbol{H}_t^0 \rangle + \langle \boldsymbol{H}_t, \mathcal{A}_3 \boldsymbol{H}_t \rangle \\ &\quad + \gamma^2 \langle \boldsymbol{H}_t, \mathcal{B} \boldsymbol{H}_t \rangle \end{aligned} \tag{12}$$

During the next process, we have two types of unknown functions in the variational formulation. One of these is $\boldsymbol{H}_t$, which we are at liberty to manipulate. The second type is $\boldsymbol{H}_t^0$, which is a disguised unknown in the sense that this particular quantity is playing the same role as the stationary solution. In other words, we must assume that $\boldsymbol{H}_t^0$ is a known function of position; this dual character must be maintained until the function is identified as that occurring at the stationary state. This constraint is to be released after extremization, making $\boldsymbol{H}_t^0 = \boldsymbol{H}_t$. It is essential to distinguish between the stationary function $\boldsymbol{H}_t^0$ and the local function $\boldsymbol{H}_t$ until the process of variation is complete, otherwise incorrect results will arise.

D. Reduction of Continuity Requirement

Equation (12) is the weak form of the boundary-value problem, but it is not suitable for ordinary nodal-based first-order finite elements which are only of C^0 continuity because the operators $\mathcal{A}_1$ and $\mathcal{A}_2$ contain second-order derivatives, requiring finite elements of C^1 continuity. However, we can remove the second-order derivatives by integration by parts. A fundamental property of finite element approximations is that they can be formulated completely locally, one element at a time, independently of the other elements. Global approximations can then be obtained by simple transformations of local equations. Based on this property, we only need to pay attention to a typical element $\bar{S}_e$ (the closure of open region S_e, $\bar{S}_e = S_e + C_e$, C_e is the boundary of $\bar{S}_e$). We also assume that the permittivity tensor inside S_e is constant. The surface integral over region S in (12) is simply the sum of the surface integrals over each element $\bar{S}_e$:

$$\int_{\bar{S}} (\bullet)\, dS = \sum_{e=1}^{N_e} \int_{\bar{S}_e} (\bullet)\, dS \tag{13}$$

where we have assumed a finite element model with N_e elements.

Performing integration by parts in (12), we arrive at a formulation which involves only first-order derivatives

$$F(\boldsymbol{H}_t) = A + \gamma^2 B \tag{14}$$

where

$$\begin{aligned} A = &\sum_{e=1}^{N_e} \int_{S_e} \epsilon_{zz}^{-1} (\nabla_t \times \boldsymbol{H}_t) \cdot (\nabla_t \times \boldsymbol{H}_t)\, dS \\ &+ \sum_{e=1}^{N_e} \oint_{C_e} \epsilon_{zz}^{-1} (\nabla_t \times \boldsymbol{H}_t) \cdot (\boldsymbol{H}_t \times \boldsymbol{n})\, dl \\ &+ \sum_{e=1}^{N_e} \int_{S_e} 2\nabla_t \cdot \boldsymbol{H}_t^0 \hat{a}_z \cdot \left\{ \nabla_t \times \left[\bar{\bar{\epsilon}}_{tt}^{-1} \cdot (\hat{a}_z \times \boldsymbol{H}_t) \right] \right\} dS \\ &+ \sum_{e=1}^{N_e} \oint_{C_e} 2\nabla_t \cdot \boldsymbol{H}_t^0 \left\{ \hat{a}_z \times \left[\bar{\bar{\epsilon}}_{tt}^{-1} \cdot (\hat{a}_z \times \boldsymbol{H}_t) \right] \right\} \cdot \boldsymbol{n}\, dl \\ &- \sum_{e=1}^{N_e} \int_{S_e} k_0^2 \boldsymbol{H}_t \cdot \boldsymbol{H}_t\, dS \end{aligned} \tag{15}$$

$$B = -\sum_{e=1}^{N_e} \int_{S_e} (\hat{a}_z \times \boldsymbol{H}_t) \cdot \left[\bar{\bar{\epsilon}}_{tt}^{-1} \cdot (\hat{a}_z \times \boldsymbol{H}_t) \right] dS \tag{16}$$

E. Variational Finite Element Formulation

In (14), the closed element boundaries C_e consist of a number of line sections which may be classified as the following two types: 1) exterior waveguide wall sections $L_e^w : L_e^w \subset C_e$ and $L_e^w \cap C = L_e^w$; and 2) interior element interface sections $L_e^i : L_e^i \subset C_e$ and $L_e^i \cap C = \emptyset$, where C is the boundary of the waveguide cross-section.

As a result, the overall contributions of the contour integral over all C_e in (14) can be rearranged as

$$\begin{aligned} \sum_{e=1}^{N_e} \oint_{C_e} &\left\{ \epsilon_{zz}^{-1} (\nabla_t \times \boldsymbol{H}_t) \cdot (\boldsymbol{H}_t \times \boldsymbol{n}) + 2\nabla_t \right. \\ &\left. \cdot \boldsymbol{H}_t^0 \left\{ \hat{a}_z \times \left[\bar{\bar{\epsilon}}_{tt}^{-1} \cdot (\hat{a}_z \times \boldsymbol{H}_t) \right] \right\} \cdot \boldsymbol{n} \right\} dl \\ &= \sum_{p=1}^{N_p} A_p^w + \sum_{q=1}^{N_q} A_q^i \end{aligned} \tag{17}$$

where

$$\begin{aligned} A_p^w = \int_{L_p^w} &\left\{ \epsilon_{zz}^{-1} (\nabla_t \times \boldsymbol{H}_t) \cdot (\boldsymbol{H}_t \times \boldsymbol{n}) \right. \\ &\left. + 2\nabla_t \cdot \boldsymbol{H}_t^0 \left\{ \hat{a}_z \times \left[\bar{\bar{\epsilon}}_{tt}^{-1} \cdot (\hat{a}_z \times \boldsymbol{H}_t) \right] \right\} \cdot \boldsymbol{n} \right\} dl \end{aligned} \tag{18}$$

$$\begin{aligned} A_q^i = \int_{L_q^i} &\left\{ \epsilon_{tt}^{-1(+)} (\nabla_t \times \boldsymbol{H}_t) \cdot \left(\boldsymbol{H}_t \times \boldsymbol{n}^{(+)} \right) \right. \\ &+ \epsilon_{zz}^{-1(-)} (\nabla_t \times \boldsymbol{H}_t) \cdot \left(\boldsymbol{H}_t \times \boldsymbol{n}^{(-)} \right) \\ &+ 2\nabla_t \cdot \boldsymbol{H}_t^0 \left\{ \hat{a}_z \times \left[\bar{\bar{\epsilon}}_{tt}^{-1(+)} \cdot (\hat{a}_z \times \boldsymbol{H}_t) \right] \right\} \cdot \boldsymbol{n}^{(+)} \\ &\left. + 2\nabla_t \cdot \boldsymbol{H}_t^0 \left\{ \hat{a}_z \times \left[\bar{\bar{\epsilon}}_{tt}^{-1(-)} \cdot (\hat{a}_z \times \boldsymbol{H}_t) \right] \right\} \cdot \boldsymbol{n}^{(-)} \right\} dl \end{aligned} \tag{19}$$

In (17), N_p is the total number of element boundary sections on the waveguide wall, N_q is the total number of interelement

boundary sections, A_p^w is the line integral contribution of the pth wall section, A_q^i is the line integral contribution of the qth interelement boundary section, the symbol $(+)$ denotes values on the interface section L_q^i from the element on one side of L_q^i, and $(-)$ denotes values on L_q^i from the element on the other side of L_q^i (as illustrated in Fig. 2).

The Line Integral on the Exterior Wall: For the first term in (18), we note from the boundary condition that $\epsilon_{tt}^{-1}\nabla_t \times \boldsymbol{H}_t$ vanishes on a PEC, and $\boldsymbol{H}_t \times \boldsymbol{n}$ vanishes on a PMC. Therefore, the contribution of $(\epsilon_{tt}^{-1}\nabla_t \times \boldsymbol{H}_t)\cdot(\boldsymbol{H}_t \times \boldsymbol{n})$ is zero on PEC, PMC, and for nonradiating modes, at infinity as well.

For the second term in (18), $\nabla_t \cdot \boldsymbol{H}_t^0$ vanishes on a PMC, and also $\{\hat{a}_z \times [\bar{\bar{\epsilon}}_{tt}^{-1} \cdot (\hat{a}_z \times \boldsymbol{H}_t)]\} \cdot \boldsymbol{n}$ will vanish on a PEC if the dielectric in the element is: i) isotropic ($\epsilon_{xy} = 0, \epsilon_{xx} = \epsilon_{yy} = \epsilon_{zz}$); or ii) uniaxial (diagonal) anisotropic ($\epsilon_{xy} = 0, \epsilon_{xx} = \epsilon_{yy} \neq \epsilon_{zz}$); or iii) of arbitrary diagonal anisotropy (only $\epsilon_{xy} = 0$), but with the element edge in the x or y direction.

Summarizing the above, we arrive at the following expression for the line integral:

$$A_p^w = \int_{L_p^w} \left\{ \epsilon_{zz}^{-1}(\nabla_t \times \boldsymbol{H}_t)\cdot(\boldsymbol{H}_t \times \boldsymbol{n}) + 2\nabla_t \cdot \boldsymbol{H}_t^0 \left\{ \hat{a}_z \times \left[\bar{\bar{\epsilon}}_{tt}^{-1} \cdot (\hat{a}_z \times \boldsymbol{H}_t) \right] \right\} \cdot \boldsymbol{n} \right\} dl = \begin{cases} 0, & \text{if } L_p^w \text{ is on PMC, PEC*, INF;} \\ \int_{L_p^w} 2\nabla_t \cdot \boldsymbol{H}_t^0 \left\{ \hat{a}_z \times \left[\bar{\bar{\epsilon}}_{tt}^{-1} \cdot (\hat{a}_z \times \boldsymbol{H}_t) \right] \right\} \cdot \boldsymbol{n}\, dl, & \text{otherwise} \end{cases} \tag{20}$$

where * means in the cases i)–iii) above.

Because the line integrals A_p^w can only be nonzero on PEC, and only when none of the above conditions i)–iii) is satisfied, we can write $A_p^w = A_p^{pec}, L_p^w = L_p^{pec}$, and reduce N_p to the number of boundary sections on a PEC satisfying none of the cases i)–iii) above.

The Line Integral on Interelement Interfaces: Note that in (19), the interelement interface unit normal vectors $\boldsymbol{n}^{(+)}$ and $\boldsymbol{n}^{(-)}$ from both sides of the interface L_q^i are precisely opposite in direction for any point on L_q^i, namely, $\boldsymbol{n}^{(-)} = -\boldsymbol{n}^{(+)}$. Additionally, from the field boundary conditions, we have $\epsilon_{zz}^{-1(+)}\nabla_t \times \boldsymbol{H}_t = \epsilon_{zz}^{-1(-)}\nabla_t \times \boldsymbol{H}_t$. Hence, the first two terms in (19) will cancel each other, reducing A_q^i to

$$A_q^i = \int_{L_q^i} 2\nabla_t \cdot \boldsymbol{H}_t^0 \left\{ \hat{a}_z \times \left[\left(\bar{\bar{\epsilon}}_{tt}^{-1(+)} - \bar{\bar{\epsilon}}_{tt}^{-1(-)} \right) \cdot (\hat{a}_z \times \boldsymbol{H}_t) \right] \right\} \cdot \boldsymbol{n}^{(+)}\, dl. \tag{21}$$

The above line integral will not vanish only if $\bar{\bar{\epsilon}}_{tt}^{-1(+)} \neq \bar{\bar{\epsilon}}_{tt}^{-1(-)}$. We therefore only need to take into account the line integral A_q^i on interfaces between different dielectrics.

Summarizing the above discussion, we finally obtain the finite element variational formulation

$$\prod = A + \gamma^2 B = 0 \tag{22}$$

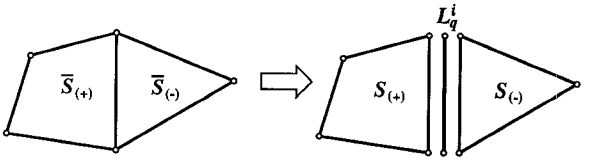

Fig. 2. Interelement interface.

where

$$\begin{aligned} A = &\sum_{e=1}^{N_e} \int_{S_e} \epsilon_{zz}^{-1}(\nabla_t \times \boldsymbol{H}_t)\cdot(\nabla_t \times \boldsymbol{H}_t)\, dS \\ &+ \sum_{e=1}^{N_e} \int_{S_e} 2\nabla_t \cdot \boldsymbol{H}_t^0 \hat{a}_z \cdot \nabla_t \times \left[\bar{\bar{\epsilon}}_{tt}^{-1} \cdot (\hat{a}_z \times \boldsymbol{H}_t) \right] dS \\ &- \sum_{e=1}^{N_e} \int_{S_e} k_0^2 \boldsymbol{H}_t \cdot \boldsymbol{H}_t\, dS \\ &+ \sum_{p=1}^{N_p^*} \delta_p^w \int_{L_p^{pec}} 2\nabla_t \cdot \boldsymbol{H}_t^0 \left\{ \hat{a}_z \times \left[\bar{\bar{\epsilon}}_{tt}^{-1} \cdot (\hat{a}_z \times \boldsymbol{H}_t) \right] \right\} \cdot \boldsymbol{n}\, dl \\ &+ \sum_{q=1}^{N_q^*} \int_{L_q^{int}} 2\nabla_t \cdot \boldsymbol{H}_t^0 \left\{ \hat{a}_z \times \left[\left(\bar{\bar{\epsilon}}_{tt}^{-1(+)} - \bar{\bar{\epsilon}}_{tt}^{-1(-)} \right) \cdot (\hat{a}_z \times \boldsymbol{H}_t) \right] \right\} \cdot \boldsymbol{n}^{(+)}\, dl \end{aligned} \tag{23}$$

$$B = -\sum_{e=1}^{N_e} \int_{S_e} (\hat{a}_z \times \boldsymbol{H}_t) \cdot \left[\bar{\bar{\epsilon}}_{tt}^{-1} \cdot (\hat{a}_z \times \boldsymbol{H}_t) \right] dS \tag{24}$$

where N_e, N_p^*, and N_q^* are the total number of elements, number of PEC boundary sections, and dielectric interface line segments, respectively. δ_p^w is defined as

$$\delta_p^w = \begin{cases} 0, & \text{in one of the cases i) – iii);} \\ 1, & \text{otherwise.} \end{cases} \tag{25}$$

F. Finite Element Implementation

Extremizing the variational finite element formulation (22) and releasing the constraint on $\boldsymbol{H}_t^0$ (making $\boldsymbol{H}_t^0 = \boldsymbol{H}_t$) leads to a matrix eigensystem of the canonical form

$$[Q]\{x\} = \lambda[R]\{x\} \tag{26}$$

where the matrices $[Q]$ and $[R]$ are, in general, large and sparse. The matrices are also nonsymmetric in the presence of dielectric inhomogeneity and/or anisotropy. Furthermore, the matrix elements are complex (and so are the eigenvalues) in the case of lossy dielectrics. For the lossless case, both matrices in (26) are real but the eigenvalues and eigenvectors can still possibly be complex conjugate (as in the case of complex modes in lossless guides).

At present, there are no standard library routines to solve this type of problem efficiently [24]–[26]. An efficient solver based on the subspace iteration algorithm, and taking full advantage of the sparsity of the matrices, has been specially developed

for this problem [20]. This solver allows us to find one or a group of eigenvalues (and the corresponding eigenvectors) closest to a given value. A preliminary implementation of our program is based on rectangular finite elements with bilinear shape functions. This choice of elements and shape functions is made to improve the accuracy of the line integral terms. The extension to arbitrary quadrilateral elements, capable of providing as much flexibility as that obtained with triangles, is straightforward [27]. Moreover, the use of quadrilateral elements, which are actually linear isoparametric elements, makes it easier to extend to (quadratic) isoparametric elements, which is more suitable to follow arbitrary curves.

III. Computational Results

In order to demonstrate the effectiveness of the method described above, we present in this section a series of examples of inhomogeneous waveguides including isotropic and anisotropic, lossless and lossy waveguides. All computations were carried out on a SUN SPARCstation 2.

A. An Optical Buried Isotropic Lossless Waveguide

Fig. 3 shows the dispersion characteristics for the E^x_{mn} and E^y_{mn} modes of an isotropic rectangular dielectric waveguide of height t and width w buried in a medium with a refractive index n_2 of 1.0; the refractive index n_1 of the guide core is 1.5. The dispersion curves are drawn in terms of the normalized index b and normalized frequency ν, which are defined by

$$b = \frac{(\beta/k_0)^2 - n_2^2}{n_1^2 - n_2^2} \tag{27}$$

$$\nu = \frac{k_0 t}{\pi}\sqrt{n_1^2 - n_2^2}. \tag{28}$$

We compare our solutions to the results of Goell [30], showing excellent agreement even at low frequency. Goell's solution is derived from cylindrical harmonic analysis, and has often been used as a benchmark for comparison in the literature [6]. However, a finite element solution is more versatile and flexible than Goell's method.

This problem is particularly sensitive to the treatment of the open boundary, especially at low frequencies. A simple truncation at a certain distance with artificial conducting walls enclosing the dielectric core can give some reasonable results at high frequency, but will fail in the lower frequency range unless a very large cross section is used in the analysis. Instead of that rather crude approach, we have used infinite elements [28], [29], in this example, to extend a fixed finite element area of dimension $(w + w) \times (t + w)$ to infinity. This gives substantially better results in the lower frequency range (in this example, for $\nu < 0.5$). Taking advantage of the symmetry, only one-quarter of the cross section has been considered, dividing that region into 456 rectangular elements. With different choices for the boundary conditions on the symmetry walls, all modes of the guide can be found. The memory requirement is less than 3 MB and the CPU time is about 35 s for each frequency on the dispersion curve.

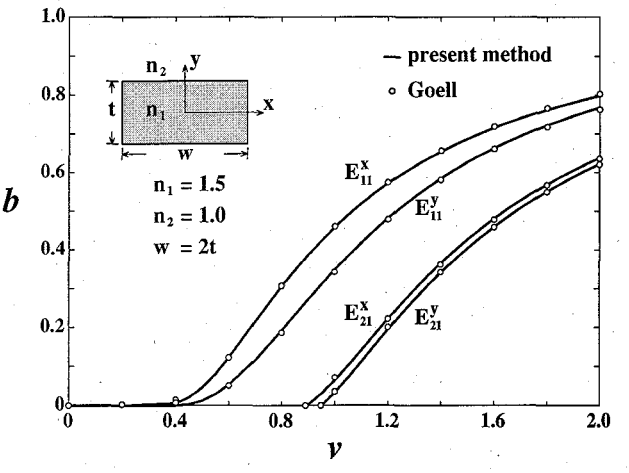

Fig. 3. Dispersion characteristics of the four lowest modes in an isotropic rectangular dielectric waveguide.

B. A Dielectric Buried Anisotropic Waveguide

Fig. 4 shows the dispersion characteristics of the four lowest modes of an anisotropic, lossless dielectric buried waveguide of rectangular cross section of height t, width $w = 2t$, core permittivity $n_x^2 = n_z^2 = 2.31, n_y^2 = 2.19$, and cladding permittivity $n_2^2 = 2.05$. Our results agree very well with those obtained by Ohtaka [31]. Ohtaka's results are obtained using a variational method and an expansion in terms of cylindrical-harmonic functions, and have been used frequently as a standard for comparison. Similarly to the example of the isotropic rectangular dielectric waveguide in Fig. 3, the use of infinite elements greatly improves the accuracy of the solution in the lower frequency range ($k_0 t < 3.5$), giving better results than Hayata *et al.* [6] and Chew and Nasir [8]. The finite element area and the mesh used in this example are the same as those used in the previous example.

C. A Lossy Rectangular Waveguide

A rectangular metallic waveguide filled with homogeneous, isotropic, and lossy dielectric is analyzed next, and the results are compared to those obtained analytically. The dielectric has a relative permittivity $\epsilon = 1.5 - j1.5$. Fig. 5 shows the relative error of the finite element solutions for the propagation constant of the fundamental TE_{10} and the next higher order TE_{01} modes in the guide, as a function of the number of mesh points. Six uniform meshes of first-order square elements, in geometric progression ($4 \times 2, 8 \times 4, 16 \times 8, 32 \times 16, 64 \times 32$, and 128×64), are used in the numerical computations. The statistics of CPU time and memory for this example are shown in Figs. 7 and 8.

The relative error e is defined by

$$e = \begin{cases} (\alpha - \bar{\alpha})/\bar{\alpha}, & \text{for the attenuation constant;} \\ (\beta - \bar{\beta})/\bar{\beta}, & \text{for the phase constant} \end{cases} \tag{29}$$

where (α, β) and $(\bar{\alpha}, \bar{\beta})$ are the finite element and exact solutions, respectively. The exact solutions are given by

$$\gamma = \alpha + j\beta = k_0\sqrt{\left(\frac{m\pi}{k_0 a}\right)^2 + \left(\frac{n\pi}{k_0 b}\right)^2 - \epsilon' + j\epsilon''} \tag{30}$$

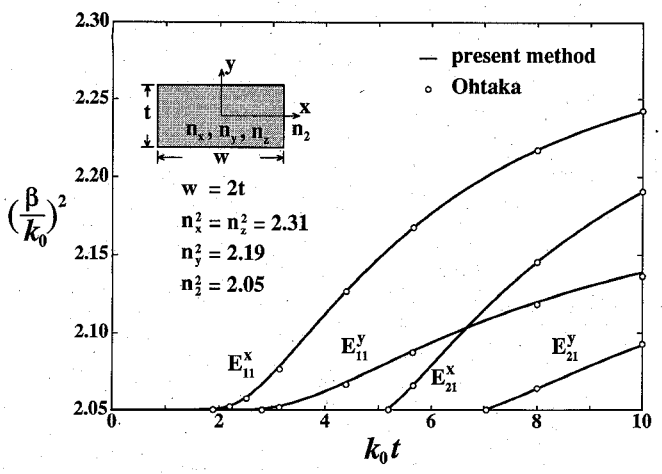

Fig. 4. Dispersion characteristics of the four lowest modes in an anisotropic rectangular dielectric waveguide.

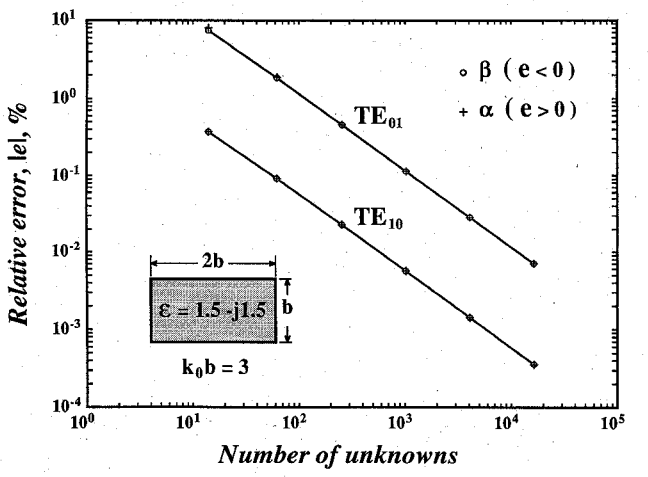

Fig. 5. Relative error of the finite element solutions for the propagation constant of the fundamental TE_{10} mode and the TE_{01} mode in a lossy dielectric-loaded metallic rectangular waveguide (inset) as a function of the number of unknowns.

where m and n are the mode indices for the x and y directions, respectively.

Fig. 5 shows that the relative error decreases as the number of unknowns increases. It is also interesting to note that the directions of convergence are opposite for the real and imaginary parts of the propagation constant; i.e., $e > 0$ for α, whereas $e < 0$ for β.

The choice of meshes in geometric progression allows for the use of the Aitken's δ^2 extrapolation method [32]. Extrapolated values taking three successive meshes are shown in Table I with the relative error in percent shown in brackets. The high accuracy of the extrapolated results, even using relatively coarse meshes, is an indication of the quality of convergence of the method.

D. An Anisotropic and Lossy Image Waveguide

The next example illustrates the case of a lossy anisotropic waveguide. Dispersion characteristics of the E_{11}^y mode in the slow wave region of an image waveguide are shown in Fig. 6, taking the real part of $\epsilon_{yy}, \epsilon'_{yy}$ as a parameter. The results in Fig. 6 compare very favorable to those obtained by Hayata *et al.* [7], needing less computer resources and showing greater accuracy than those. Similar advantages are observed in the calculation of the dispersion characteristics as a function of the loss parameter [7], [19]. Our results were obtained on a SUN SPARCstation 2 requiring about 17 s CPU time for each frequency and less than 2.5 MB of memory to solve the above problem using a mesh of first order rectangular elements and 625 nodes. It is interesting to note that the results of Hayata *et al.* were obtained using a mesh of only 81 nodes but requiring 7.6 MB of memory and 10 s of CPU time in a Hitachi S-810/10 supercomputer [7].

The resultant matrix problem in this as in all cases of inhomogeneous and/or anisotropic dielectrics consists of large non-Hermitian matrices. The matrix solver mentioned before allows a very efficient and fast solution as dramatically illustrated in Figs. 7 and 8 showing statistics of CPU time and storage for the lossy waveguide problem described in Fig. 5. The performance of our sparse matrix solver is here compared against the complex matrix routine F02GJF from the NAG library [25]. The dense-matrix QZ algorithm (on which that routine is based) is the only one available for this type of problem in standard computer libraries [25], [26].

The order of the resultant matrices, denoted by N_m, is twice the number of nodal points in the mesh. After applying boundary conditions, the number of actual unknown values reduce to N_u, the order of the matrix problem to solve. Empirical expressions can be fitted to the measured CPU time t_{s1} and the estimated memory requirements m_{s1} as functions of N_u and N_m, respectively.

$$t_{s1} \approx 4.3 \cdot 10^{-4} N_u^{1.5} \text{ (seconds)} \tag{31}$$

$$m_{s1} \approx 1.85 N_m \text{ (kilobytes)}. \tag{32}$$

When referring to CPU time, N_u is more representative than the number of nodes, while in connection to memory requirements, N_m is more adequate. In our formulation, $N_m = 2N_p, N_u \leq N_m$.

The exact values of the parameters in the fitting will vary slightly for different problems but these results clearly show that a sparse-matrix solver of this kind will drastically reduce CPU time and memory requirements to be proportional to about $N^{1.5}$ and N, respectively, while for a dense-matrix algorithm they would be proportional to N^3 and N^2, respectively. The sparse matrix eigenvalue solver enables this method to solve problems with more than 10 thousand unknowns in reasonable time on a medium-size workstation.

Computational results of all the examples shown are very satisfactory. No spurious solutions appear in any of the examples which cover all categories of dielectric waveguide problems—lossless isotropic, lossless anisotropic, lossy isotropic, and lossy anisotropic dielectric waveguides including both closed and open structures. Furthermore, the fact that the resultant matrix problem is non-Hermitian in the case of inhomogeneous guides (even for the lossless case), far from being a deficiency of this formulation, shows its completeness, in allowing the analysis of complex modes in lossless guides [20].

TABLE I
EXTRAPOLATED RESULTS AND THEIR RELATIVE ERRORS

Meshes	TE_{10} mode		TE_{01} mode	
	α/k (e, %)	β/k (e, %)	α/k (e, %)	β/k (e, %)
1, 2, 3	0.59638493 (4.9E-4)	1.2575780 (-4.1E-4)	0.75852665 (3.5E-2)	0.98909351 (-1.4E-3)
2, 3, 4	0.59638217 (3.4E-5)	1.2575830 (-2.7E-5)	0.75828594 (3.5E-3)	0.98909317 (-1.4E-3)
3, 4, 5	0.59638198 (3.5E-6)	1.2575832 (-6.1E-6)	0.75826094 (2.3E-4)	0.98910670 (-1.0E-4)
4, 5, 6	0.59638196 (1.9E-7)	1.2575833 (-2.6E-7)	0.75825924 (1.4E-5)	0.98910770 (-8.0E-6)
Exact	0.596381963112	1.257583304643	0.758259127827	0.989107776585

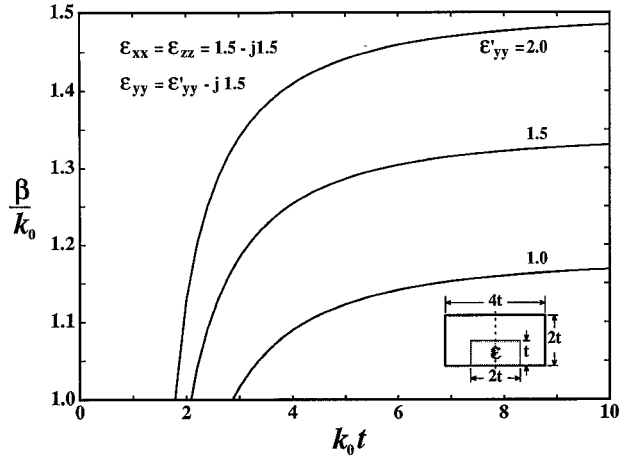

(a)

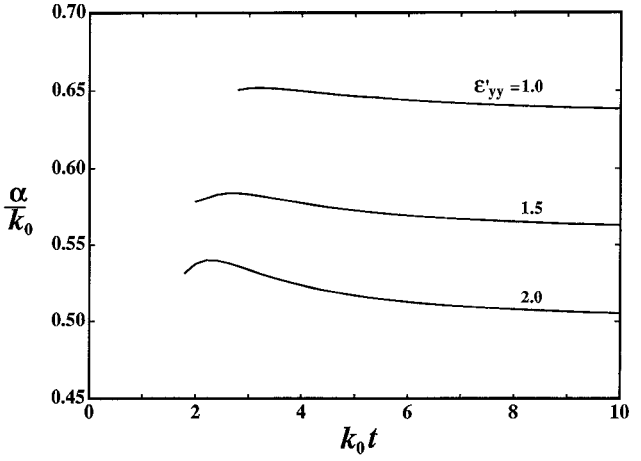

(b)

Fig. 6. Dispersion characteristics of the E_{11}^y mode in a shielded image waveguide with anisotropic lossy dielectric. (a) Normalized phase constant. (b) Normalized attenuation constant.

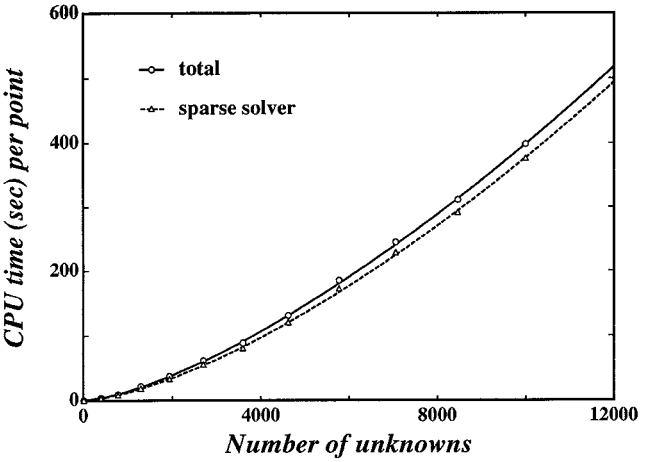

Fig. 7. CPU time for the lossy waveguide problem shown in Fig. 5 using the sparse matrix solver on a SUN SPARCstation 2.

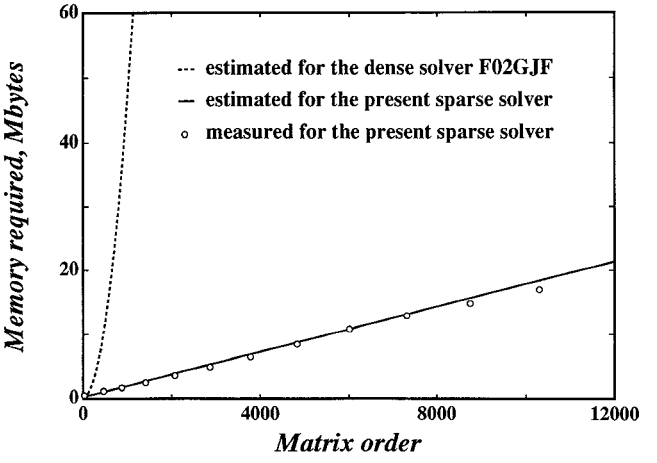

Fig. 8. Comparison of memory requirements from the sparse matrix solver using a subspace of order 1 and its NAG equivalent complex dense-matrix routine F02GJF.

IV. CONCLUSIONS

A variational finite element method for the analysis of microwave and optical waveguide problems with arbitrary cross section and inhomogeneous, anisotropic, and lossy dielectrics has been described in detail. With this approach, solutions are obtained directly for complex propagation constants. Spurious solutions are totally eliminated by explicitly including the divergence-free condition for the magnetic field in the formulation. This is achieved by the elimination of the longitudinal component of the magnetic field, leaving a very efficient representation of the problem in terms of the two transverse components only.

The resultant matrix eigenvalue problem is of canonical form and, although the matrices are non-Hermitian in the general case, preventing the use of standard library packages, an efficient solver has been developed specially for this formulation taking full advantage of the sparsity of the matrices. This solver allows to find very efficiently one or a group of eigenvalues (and the corresponding eigenvectors) at a time. The order of the matrices is at most twice the number of mesh

nodes and the sparsity depends only on the topology of the mesh.

This method has been thoroughly tested solving a comprehensive range of guiding structures in microwaves and optics, and examples are given here that include isotropic and anisotropic, lossless and lossy dielectric waveguides, as well as both closed and open-boundary structures. The numerical results compare very well to those obtained by other methods.

ACKNOWLEDGMENT

The authors would like to thank Prof. P. C. Kendall, Prof. J. B. Davies for stimulating discussions and helpful suggestions, and Shou-Zheng Zhu for his contribution to the development of the sparse matrix eigenvalue solver.

REFERENCES

[1] J. B. Davies, F. A. Fernandez, and G. Y. Philippou, "Finite element analysis of all modes in cavities with circular symmetry," *IEEE Trans. Microwave Theory Tech.*, vol. MTT-30, pp. 1975–1980, Nov. 1982.

[2] B. M. A. Rahman and J. B. Davies, "Finite-element analysis of optical and microwave waveguide problems," *IEEE Trans. Microwave Theory Tech.*, vol. MTT-32, pp. 20–28, Jan. 1984.

[3] C. G. Williams and G. K. Cambrell, "Numerical solution of surface waveguide modes using transverse field components," *IEEE Trans. Microwave Theory Tech.*, vol. MTT-22, pp. 329–330, Mar. 1974.

[4] J. B. Davies, F. A. Fernandez, and Y. Fang, "Finite-difference solution of inhomogeneous waveguide modes using a fast direct solver routine," *IEEE Trans. Magnetics*, vol. MAG-27, pp. 4028–4031, Sept. 1991.

[5] B. M. A. Rahman and J. B. Davies, "Penalty function improvement of waveguide solution by finite elements," *IEEE Trans. Microwave Theory Tech.*, vol. MTT-32, pp. 922–928, Aug. 1984.

[6] K. Hayata, M. Koshiba, M. Eguchi, and M. Suzuki, "Vectorial finite-element method without any spurious solution for dielectric waveguiding problems using transverse magnetic-field component," *IEEE Trans. Microwave Theory Tech.*, vol. MTT-34, pp. 1120–1124, Nov. 1986.

[7] K. Hayata, K. Miura, and M. Koshiba, "Finite-element formulation for lossy waveguides," *IEEE Trans. Microwave Theory Tech.*, vol. MTT-36, pp. 268–276, Feb. 1988.

[8] W. C. Chew and M. A. Nasir, "A variational analysis of anisotropic, inhomogeneous dielectric waveguides," *IEEE Trans. Microwave Tech.*, vol. MTT-37, pp. 661–668, Apr. 1989.

[9] J. A. M. Svedin, "A numerically efficient finite-element formulation for the general waveguide problem without spurious modes," *IEEE Trans. Microwave Theory Tech.*, vol. MTT-37, pp. 1708–1715, Nov. 1989.

[10] I. Bardi and O. Biro, "An efficient finite-element formulation without spurious modes for anisotropic waveguides," *IEEE Trans. Microwave Theory Tech.*, vol. MTT-39, pp. 1133–1139, July 1991.

[11] C. F. Bryant, B. Dillon, C. R. I. Emson, J. Simkin, and C. W. Trowbridge, "Solving high frequency problems using the magnetic vector potential with Lorentz gauge," *IEEE Trans. Magnetics*, vol. 28, pp. 1182–1185, Mar. 1992.

[12] A. Bossavit and I. Mayergoyz, "Edge-elements for scattering problems," *IEEE Trans. Magnetics*, vol. MAG-25, pp. 2816–2821, July 1989.

[13] J. F. Lee, D. K. Sun, and Z. J. Cendes, "Tangential vector finite element for electromagnetic field computation," *IEEE Trans. Magnetics*, vol. MAG-27, pp. 4032–4035, Sept. 1991.

[14] ——, "Full-wave analysis of dielectric waveguides using tangential vector finite elements," *IEEE Trans. Microwave Theory Tech.*, vol. MTT-39, pp. 1262–1271, Aug. 1991.

[15] M. Koshiba and K. Inoue, "Simple and efficient finite-element analysis of microwave and optical waveguides," *IEEE Trans. Microwave Theory Tech.*, vol. MTT-40, pp. 371–377, Feb. 1992.

[16] R. Miniowitz and J. P. Webb, "Covariant-projection quadrilateral elements for the analysis of waveguides with sharp edges," *IEEE Trans. Microwave Theory Tech.*, vol. MTT-39, pp. 501–505, Mar. 1991.

[17] F. A. Fernandez and Y. Lu, "Variational finite element analysis of dielectric waveguides with no spurious solutions," *Electron. Lett.*, vol. 26, pp. 2125–2126, Dec. 1990.

[18] ——, "A variational finite element formulation for dielectric waveguides in terms of transverse magnetic fields," *IEEE Trans. Magnetics*, vol. 27, pp. 3864–3867, Sept. 1991.

[19] Y. Lu and F. A. Fernandez, "A new variational finite element analysis of microwave and optical waveguides without spurious solutions," in *Proc. IEE Int. Conf. Computat. Electromagnetics*, London, UK, Nov. 25–27, 1991, pp. 160–163.

[20] F. A. Fernandez, J. B. Davies, S. Zhu, and Y. Lu, "Sparse matrix eigenvalue solver for finite element solution of dielectric waveguides," *Electron. Lett.*, vol. 27, no. 26, pp. 1824–1826, Sept. 1991.

[21] R. E. Collin, *Field Theory of Guided Waves.* New York: IEEE Press, 1991.

[22] C. H. Chen and C. D. Lien, "The variational principle for non-self-adjoint electromagnetic problems," *IEEE Trans. Microwave Theory Tech.*, vol. MTT-28, pp. 878–886, Aug. 1980.

[23] R. S. Schechter, *The Variational Method in Engineering.* New York: McGraw-Hill, 1967.

[24] B. T. Smith *et al.*, *Matrix Eigensystem Routines—EISPACK Guide.* New York: Springer-Verlag, 1976.

[25] *NAG Fortran Library,* Numerical Algorithms Group Ltd., Oxford, UK, 1991.

[26] *IMSL Fortran Math/Library,* IMSL Inc., TX, 1991.

[27] T. J. R. Hughes, *The Finite Element Method—Linear Static and Dynamic Finite Element Analysis.* Englewood Cliffs, NJ: Prentice-Hall, 1987.

[28] P. Bettess, "Infinite elements," *Int. J. Numer. Meth. Eng.*, vol. 11, pp. 53–64, 1977.

[29] P. Bettess, "More on infinite elements," *Int. J. Numer. Meth. Eng.*, vol. 15, pp. 1613–1629, 1980.

[30] J. E. Goell, "A circular-harmonic computer analysis of rectangular dielectric waveguides," *Bell Syst. Tech. J.*, vol. 48, pp. 2133–2160, Sept. 1969.

[31] M. Ohtaka, "Analysis of the guided modes in the anisotropic dielectric rectangular waveguides" (in Japanese), *Trans. Inst. Electron. Commun. Eng. Japan*, vol. J64-C, pp. 674–681, Oct. 1981.

[32] J. Stoer and R. Bulirsch, *Introduction to Numerical Analysis.* New York: Springer-Verlag, 1980.

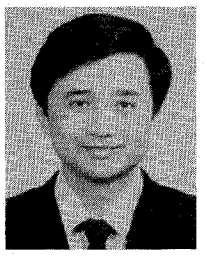

Yilong Lu was born in Chengdu, China, in 1958. He received the B. Eng. degree from Harbin Institute of Technology, Harbin, China, in 1982, and the M. Eng. degree from Tsinghua University, Beijing, China, in 1984. He received the Ph.D. degree from University College London, London, UK, in 1991, all in electronic engineering.

From 1984 to 1988 he was with the Department of Electromagnetic Fields Engineering, the University of Electronic Science and Technology of China, Chengdu, China. He joined Nanyang Technological University, Singapore, in 1991 where he is currently a Lecturer in the School of Electrical and Electronic Engineering. His current research interests include finite element methods for modeling microwave and optical components, antenna CAD, and application of numerical techniques for electromagnetic problems.

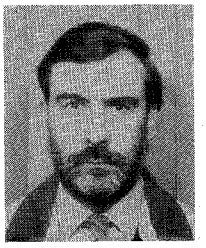

F. Anibal Fernandez was born in Santiago, Chile, in 1945. He received the Ingeniero Matematico degree from the Universidad de Chile in Santiago in 1969. From 1970 to 1985 he was on the academic staff of the Department of Electrical Engineering, Universidad de Chile in Santiago, with the exception of three years spent at University College, London, where he received the Ph.D. degree in electrical engineering in 1981.

In 1986 he joined the staff of the Department of Electronic and Electrical Engineering, University College London, England. Current research interests include aspects of electromagnetic field theory, microwaves, nonlinear optics, and especially the use of numerical methods in those fields.